

# Using seismic hazard assessment to study dynamic behavior of Gonbad-e Kāvus tower (the tallest brick tower in the world)

Gholamreza Ahmadi · Rooholla Keshtkar ·  
Masoud Mavizchi · Mohammad Ghasem Vetr

Received: 8 April 2014 / Accepted: 3 November 2014 / Published online: 19 November 2014  
© The Author(s) 2014. This article is published with open access at Springerlink.com

**Abstract** Gonbad-e Kāvus Brick tower, which was completed in the tenth century, is the remnant of an ancient glorious building that is located in downtown of Gonbad-e Kāvus, Golestan, Iran. It is of note that, this massive brick structure is known as the tallest brick tower in the world. Unfortunately, the tower is located on a very active seismic region, hence there is an urgent need for a careful study of seismic behavior of the tower due to its historical importance. Hence, probabilistic seismic hazard assessment has been performed for Gonbad region to prepare the acceleration spectrum charts. Three-dimensional finite element models of the tower are used in the nonlinear finite element program ANSYS. Dynamic modal and dynamic analyses by means of two spectral accelerations were conducted to study the dynamic response. In conclusion, earthquake with 2,475 years period duration can cause damage to the overall the tower.

**Keywords** Historical masonry tower · Three-dimensional finite element model · Dynamic response · Probabilistic seismic hazard assessment

## Introduction

Most of the existing historical monumental structures are made of masonry, using either stone or brick blocks. These unreinforced blocky masonry structures cannot be considered a continuum, but rather an assemblage of compact stone or brick elements linked by means of mortar joints. Seismic events have often caused massive damage or the destruction of such structures with great cultural significance.

The main purpose of the current study is analysis of the seismic response of large monumental masonry. The specific size and geometry of the old structures and also specific architectural parts such as large facades, arches and vaults are often the main reasons for presence of seismic damages even in a moderate earthquake. On the other hand, the same structures of Gonbad-e Kāvus brick tower are special type of the Iranian architectural heritage.

Kāvus tower of Gonbad-e Kāvus, Golestan Province, is an outstanding and innovative example of Islamic architecture with the 52.07 m height body that is registered on UNESCO's heritage list with international monuments registration number of 1398 and also this is known as the tallest brick tower in the world in 2012. Besides, Gonbad-e Kāvus known as Gonbad-e Ghābus, is a monument related to the fourth century A.H. that was built in 1006 AD on the order of Ziyarid ruler, Shams-ol-Ma'ali Qābus ibn Voshmgir, and is near the ruins of the ancient city of Jorjan in the northeast Iran located on a hillock amidst the grand park of the city (Fig. 1).

---

G. Ahmadi (✉) · M. Mavizchi  
Department of Civil Engineering, Islamic Azad University, Yazd  
Branch, Yazd, Iran  
e-mail: grahmadi@hotmail.com

M. Mavizchi  
e-mail: m.mavizchi@iauyazd.ac.ir

R. Keshtkar  
Applied-Scientific University of Golestan, Gorgan, Iran  
e-mail: enkeshtkar@yahoo.com

M. G. Vetr  
Structural Research Center, International Institute of Earthquake  
Engineering and Seismology (IIEES), Tehran, Iran  
e-mail: vetr@iiees.ac.ir



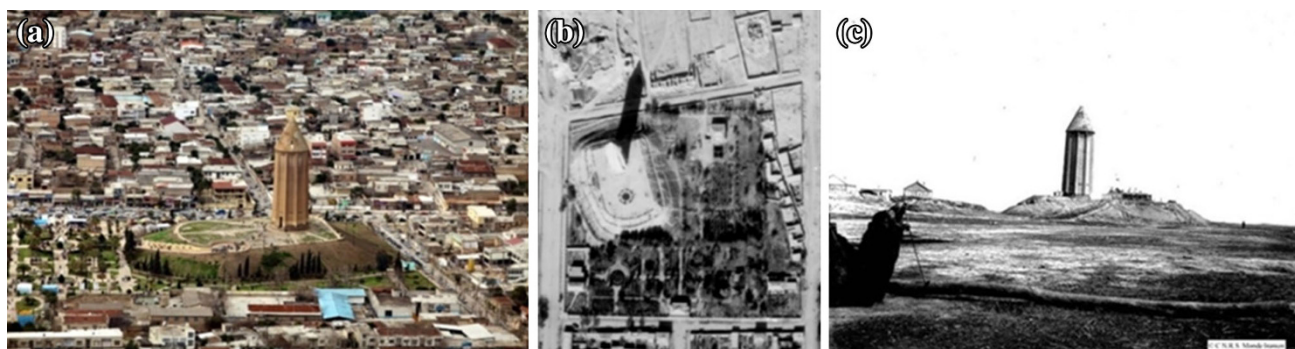


**Fig. 1** **a** Gonbad-e Kāvus tower location; **b** aerial photo taken on 1335; **c** Gonbad-e Kāvus in the 1950s



**Fig. 2** **a** The destruction of the lower part of the tower due to find the treasure; **b** reconstruction of the damaged part in the lower part of the tower; **c** reconstruction of the damaged part in the *cone-shaped* dome

Since Iran is located on one of the world's seismic lines, Gonbad-e Kāvus tower is located in an area with relatively high risk of earthquake. Knowing the fact that it is a historical structure with considerable age, we feel the necessity to study the region with risk analysis method and to obtain two specific spectra of the site with periods of 475 and 2,475 years for understanding the seismic behavior of Gonbad-e Kāvus tower. After obtaining two site-specific spectra, a finite elements model is defined with the non-linear finite elements software ANSYS, and subsequently the features, properties and other required parameters are presented.

According to the available evidences, this massive masonry structure has been under threat and harmed severely by natural and unnatural factors. People in earlier times have damaged the body of the structure since they thought there was treasure buried at the surrounding of the foundation of the structure, thus imposing slight damages to this tower (Fig. 2a). During the times there have been implementations for repairing according to Fig. 2b, c, the empty holes have been filled using similar bricks, and old bricks have been removed and new ones have been used, this action has hidden the deeper cracks from sight.

## Literature review

In the far past, historic monuments were built by the ancestors and forefathers, besides the historical value it represents civilization, culture and abilities of past people. Moreover, another factor that increased the importance of protecting these buildings is the monument's role in job creation and economic interests of the countries. Note that, Iran is one of the top ten countries in the world in terms of historical attractions. Therefore, adopting appropriate solutions is necessary in order to protect the historic monuments against demolition. In order to improve the historic buildings against earthquakes, a full evaluation of the building is needed to identify the structural properties of the historic buildings. Gonbad-e Kāvus tower is a one of the historic monuments that has a global reputation. So far in addition to restoration that has been done to replace damaged parts, the studies were conducted to evaluate the seismic behavior of the tower. Among these studies, an evaluation of the tower is done by Hejazi and Nasri (2009) in linear time history analysis using Naghan earthquake accelerations. Another paper associated with this tower is a nonlinear time history analysis of the tower under the Northridge earthquake (Ahmadi et al. 2012) that evaluated retrofit of the tower with seismic isolation systems.



In the following, a review of the same work on masonry towers is presented. Since a review of all experimental and analytical studies in this regard is not possible, a summary of the related works is presented below.

The numerical damage assessment of the masonry bell tower called “Haghia Sophia” in Trabzon, Turkey, was performed by Bayraktar et al. (2010), through utilizing nonlinear static and dynamic analyses by nonlinear 3D finite element modeling. Nonlinear dynamic analysis has been performed according to east–west component of the 1992 Erzincan earthquake. A simple strategy of analysis for the seismic assessment of the Qutb Minar in Delhi, India, was presented by Peña and Lourenço (2010). Three different models were used for nonlinear static (pushover) and nonlinear dynamic analyses. A comparative numerical study on a twelfth century masonry tower called “Matildea bell tower” located in northern Italy was described by Milani et al. (2012). To assess the safety of the tower under seismic loads, different numerical analyses have been performed: nonlinear static, limit, and nonlinear full dynamic analyses. The results of an experimental campaign composed of both non-destructive static and dynamic tests on an illustrative masonry tower: the Italian Medieval “Torre Grossa” (Big Tower) of San Gimignano in Toscana (Italy) was reported and discussed by Bartoli et al. (2013). During the experimental campaign, both static and dynamic tests were performed. By using the finite element technique, a 3D model of the tower was built (macro-modeling) and it was calibrated on the basis of the in situ investigation survey. In addition to these, many useful studies have been done about old historical structures (e.g., D’Ambrisi et al. 2012; Ceroni et al. 2009; Ivorra and Pallarés 2006; Lourenço 2005; Binda et al. 2005; Carpinteri et al. 2005; Modena et al. 2002; Riva et al. 1998).

As shown in previous researches, the seismic evaluation methods include conventional static and dynamic analysis with consideration of linear and nonlinear materials. In this paper, in order to do more accurate study of the seismic behavior of the tower and also more convenient and accurate understanding of the geology, tectonic, seismology, risk and available faults, risk analysis has been used. Risk analysis helps in providing suitable acceleration spectra so that it results in a more realistic understanding of the seismic behavior of the tower.

In this regard, another important parameter is height-to-width ratio of the tower, usually in previous researches, thin ratio of most masonry towers is greater than 4. In this regard, Asinelli tower has the most height-to-width ratio equal to 11, while the Gonbad-e Kāvus tower is a load-bearing masonry structure approximately 52.07 m tall and 17.24 m width which its ratio of width to height is equal to 3 approximately so this is a sign of stability after 1,000 years. Besides, for the accuracy and simplicity of

modeling, a macro-modeling method is used in this paper by which wide range of other structures are modeled.

### Properties of the structure

This monument structure is located in a high hill that consists of two parts: the first part is the base and the body, and the second part consists of a brick conical dome. Normal red baked brick without cover has been used for both the facade and bearing of the structure and also Saruj mortar (plaster lime and ashes or sand) has been used to fill the gap among bricks.

The overall height of the structure is 52.07 m that includes the conical dome with height equal to 15.07 m and brick body with height equal to 37 m (Fig. 3a, b). In considering the height of the hill (equal to 15 m), summation of the heights of structure and underneath hill gives about 67.07 m. The foundation of the structure is a circular foundation that consists of mixture of brick and cement. The important feature about the foundation of the structure apart from its height and material is the extra volume of soil added to the surrounding of the foundation that creates a kind of pre-stressed pattern. In this research, the soil–structure interaction has been ignored. In other words, only the structure is our criterion for seismic studies. On the other hand, the very important feature of the body of the dome is its perfect symmetry (central symmetry and axial symmetry with respect to diameter of circular plan) in a way that every point of the structure has a twin point in the opposite. And also all concavities and convexities are also symmetric on the plan. The outer circular body of Gonbad-e Kāvus is in the form of a ten-pointed star to a conical roof that each corner (play the role of trailer) has equal distances from each other. The internal body is continued like a cylinder to top of the dome, and also in the southern part there is an entrance with 1.56 m of width and 5.53 m of height. Other geometric properties are presented in Fig. 3a, b by the length and cross sections.

### Numerical simulation

As shown in Fig. 4, three-dimensional finite elements models of the tower have been made with the aid of original nonlinear finite element program ANSYS. Then, meshing of the model is an initial step in a finite element analysis; hence, mesh density is considered in lower location of body structure more than other places.

Depending on the desired accuracy and simplicity, modeling can be done in different ways that in general can be divided in the form of micro-modeling and macro-modeling. The bricks are modeled greater than usual and between them is used from members and contact



**Fig. 3** Geometric relief of Gonbad-e Kāvus tower: **a** vertical section; **b** cross sections at different levels

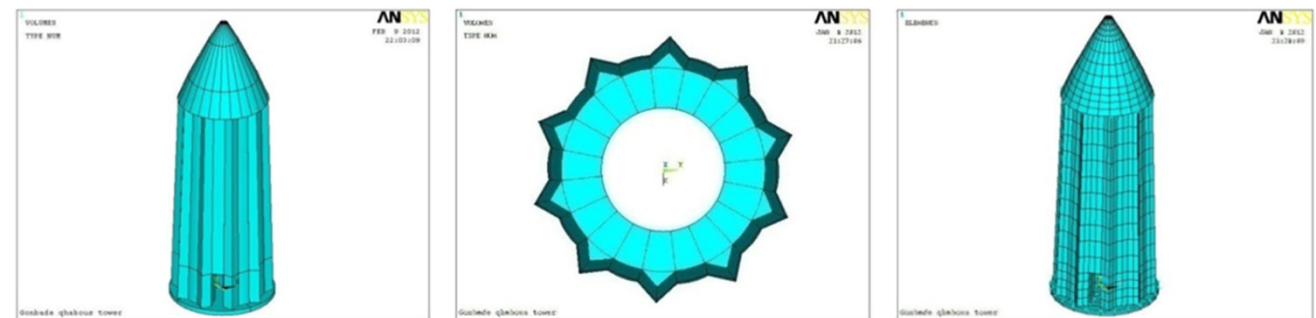
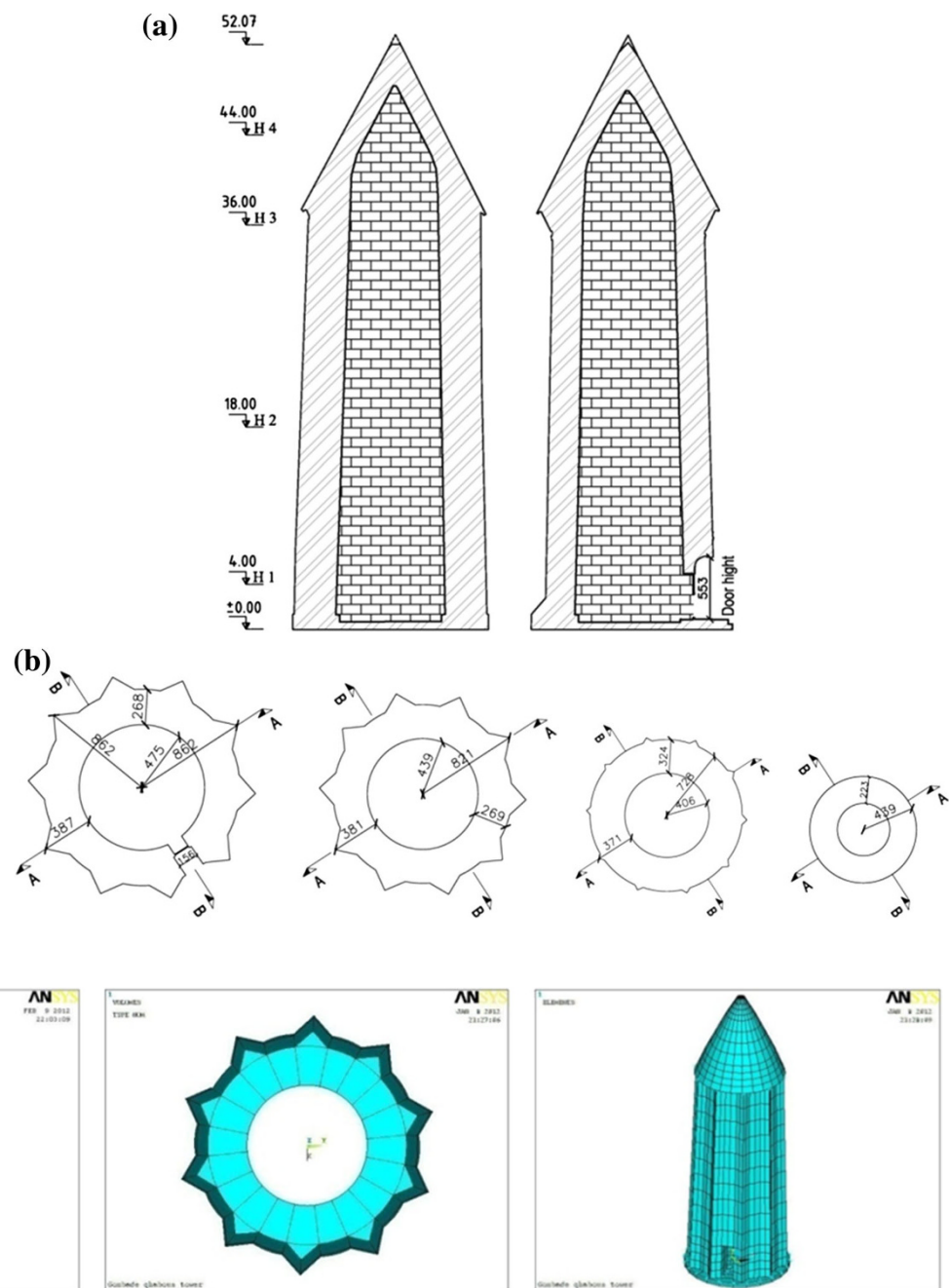


**Fig. 4** Modeling and discretization views of structure in ANSYS program

components, and in fact mortar was removed from the model and its effects will be considered in members and contact components. As a principal rule it should be noted that the modeling of the structures should, as far as does not damage the results of the study, be simple. Due to the cost and time consumed, applying micro-modeling in the seismic analysis of the structures can be used only for research and small samples. Therefore, in the modeling and investigation of the seismic behavior of the large-scale structures, a model without numerous details and

complexities of micro-modeling and provides a good representation of the overall behavior of the structures is needed. For example, in the macro-modeling method an element of the tower, with large dimensions and the volume approximately  $3 \text{ m}^3$ , has been modeled and meshed. However, if it is modeled with micro method this volume should be replaced with a large number of small elements consisting of brick and mortar ( $0.25 \times 0.25 \times 0.06 \text{ m}$ ). Hence, the advantage of macro-modeling approach compared to micro-modeling approach is in reducing the





computational time and computer disk space requirements significantly. Hence in this study, the macro-modeling approach was used, and the masonry was modeled as an isotropic continuum. Besides, three types of elements were used to model; SOLID65, CONTA175 and TARGE170 elements, in which the first element is used for wall and the second and third elements are used for taking into account the interaction between foundation and body of the building and the dome, respectively.

#### Mechanical properties of materials

Because of the sensitivity of societies and organizations and relevant administrations of historical structures preserving, we are not allowed to perform any tests whether laboratory tests or environmental tests; therefore, we are obliged to obey the instructions about seismic optimization of masonry structure and also other researches about brick structures that are similar to this ancient structure with view point of age and quality.

Therefore, we have used characteristics of Imam Reza Shrine materials and also Najmaddin Kobra monument which are located within 200 km of this structure. These two buildings have the same materials, arrangement, and age compared with Gonbad-e Kāvus tower. Parts of the foundation of Imam Reza Shrine were investigated by performing single and double-flat jack tests by Astan Quds Razavi consulting department, the results of which are mentioned in the paper of Mavizchi et al. (2012).

Hence, for brick wall, the following properties must be entered in ANSYS:

- Elastic modulus ( $E_C$ ) = 2.33 e6 KN/m<sup>2</sup>
- Ultimate uniaxial compressive strength = 3,600 KN/m<sup>2</sup>
- Ultimate uniaxial tensile strength = 170 KN/m<sup>2</sup>
- Poisson's ratio ( $\nu$ ) = 0.25
- Density ( $\rho$ ) = 1.8 ton/m<sup>3</sup>.

Also in the present study it is assumed that the concrete is homogeneous and initially isotropic. On the other hand, because of the prohibition of testing, we decided to use a laboratory sample of brick wall which was done by Nateghi-Alahi and Alemi (2008), with the purpose of calibrating the nonlinear finite element program ANSYS and to assure the proper function of the program for investigating of the modeling the brittle walls (bricks). The result of the laboratory wall sample under cyclic test is presented in Fig. 5a. The three-dimensional finite element model of the brick wall and meshed in ANSYS program is presented in Fig. 5b, c which shows the results of analysis of the brick wall. For this study the following properties were entered in ANSYS: elastic modulus ( $E_C$ ) = 5,400 kg/cm<sup>2</sup>, ultimate uniaxial compressive strength = 3,600 kg/cm<sup>2</sup>, ultimate

uniaxial tensile strength = 170 kg/cm<sup>2</sup>. As it is clear from Fig. 5c, the beginning of cracks are from the window corners and wall toes that conform to the laboratory image and represents the program accurate function from the behavior of a the brick wall.

#### Numerical analysis

##### Gravitational analysis

By doing a static analysis for gravity loads, the mechanism of load transmission between elements of the structure, the static of the structure under its own weight, and also the reliability of modeling has been determined.

In this field, although the creeping deformation of the materials which had been happening since the beginning of the construction has not been taken into account, by doing the gravity analysis and studying the results, it can be result that the structure is in a good condition, except one small part in the front side of the entrance that undergoes excessive tensile stress than the allowable value (170 KN/m<sup>2</sup>). But overall, according to Fig. 6, the structure has shown suitable resistance to compression, tensile and shear stress, and also load transmission among the elements of the structure has been done in an acceptable manner. Applying this analysis the weight of the structure is obtained as 86,400 KN.

##### Evaluation criteria of the Iranian Seismic Code (2800)

The ground motion assumptions that were applied in dynamic analysis must at least include the conditions of “design earthquake”. In fact design earthquake is an extreme earthquake with probability of occurrence, or the probability of any stronger earthquake than it, would be less than 10 % during the 50 years of useful lifetime of the structure. The effect of ground motion will be determined by one of the two ways, i.e., first by acceleration response spectrum and secondly, by time history of acceleration. For “acceleration response spectrum” either “standard design spectrum” or the “site specific design spectrum” can be used. Applying any of these methods is optional for all buildings, but where dynamic analysis is needed due to the specific conditions, applying “site specific design spectrum” will be mandatory. These specific conditions are given as follows:

1. Buildings with “high and very high importance factor” which are located on the soil type IV.
2. Buildings taller than 50 m located on soil type IV.
3. Buildings taller than 50 m located on soil types II.b and III.b, in which its thickness of the soil layer is more than 60 m.



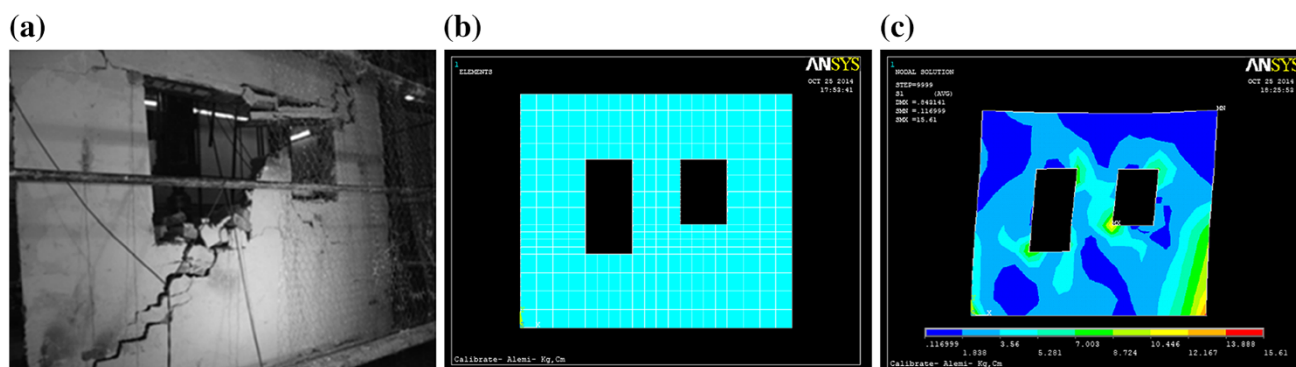


**Fig. 5** **a** The URM perforated wall with two windows after the cyclic test; **b** the three-dimensional finite element model of the brick wall; **c** the results of analysis of the brick wall

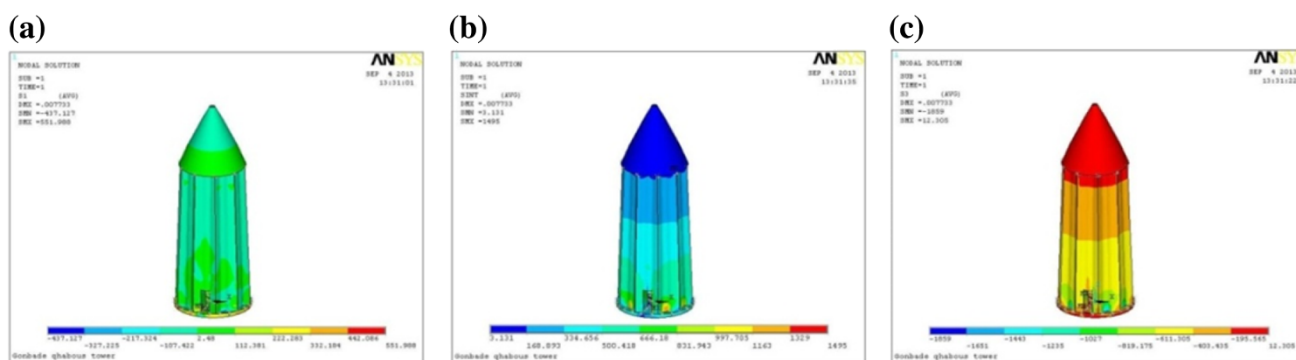


**Fig. 6** **a** Tensile stress (S1); **b** compressive stress (S3); **c** shear stress (Sint)

Gonbad-e Kāvus tower covers these conditions, so studying the effects of ground motion on the structure, applying “acceleration response spectrum” and “site specific design spectrum” is mandatory. In the current study, this spectrum is obtained by risk analysis method.

In accordance with paragraph 13 and 14 of the Iranian Seismic Code (2800), the following items should be considered for dynamic analysis of non-building structures:

1. Period time of vibration of the structure must be identified by one of known processing of analysis.
2. If the main period time of the structure is more than 0.5 s, applying one of the dynamic analysis methods is mandatory to obtain lateral forces.

#### Gonbad seismic zone

Destructive earthquakes presented in Table 1 manifests that the area comprising Gonbad-e Kāvus tower is subjected to high seismic hazards. Hence, in the current study, horizontal peak ground acceleration (PGA) values on a grid of 300 points in Golestan area were studied by modified probabilistic seismic hazard assessment. Since, according to test results, the soil of study area has closest match with

soil type III that has been introduced in the regulation for seismic design of buildings.

#### Tectonic and seismotectonic of study area

The study region, as shown in Fig. 7, is situated in three major seismotectonic provinces that are defined by Mirzaei: the Kopehdagh, the Alborz-Azarbajestan and the Central-East Iran. In order to estimate of the seismicity parameters, the procedures introduced by Kijko and Sellevollare used, which allow integration of magnitude uncertainty to estimate seismicity parameters from imperfect information documents.

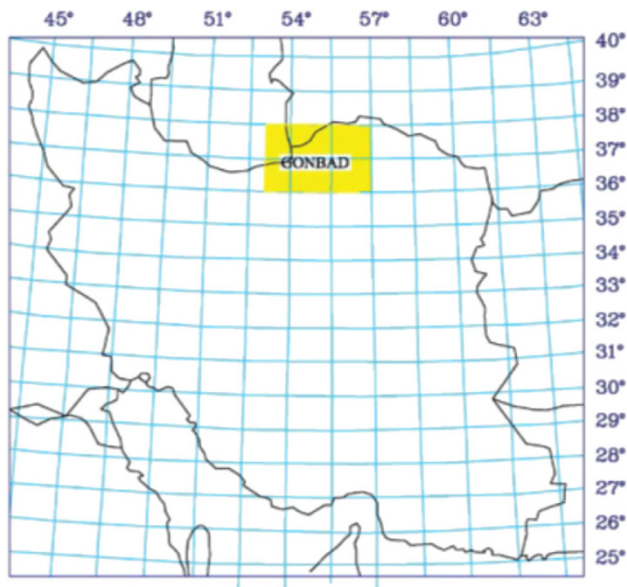
Seismicity history of Iran denotes that in the most parts of Iran, faults are identified as the principal earthquake sources. Therefore, the fundamental steps for tectonic setting are identity of the faults in the region. There are more faults around Gonbad-e Kāvus such as Astaneh fault, Damghan fault, Maiami fault, Attari fault, Radakan, Shahkooh, Talanbar and Hajiabad faults. In addition, the two crucial faults and their specifications in the study region are presented as follows:

*Khazar fault:* That is a thrust and active fault extends more than 600 km extent, an E–W curved strike from north



**Table 1** Some of destructive earthquakes in the study region

No.	Year	Location	Damage
1	874	Gorgan	2,000 soldiers dead, Gorgan's people migrated to Baghdad
2	1127	Hezar Jarib	Many villages in Farim region destroyed
3	1301	South Mazandaran	Many villages in South Mazandaran destroyed, economical damage in Farim region
4	1470	Gorgan	A village near Abeskun region disappeared
5	1498	Gorgan	Thousands of people dead, many houses destroyed
6	1809	Shirgah-Ganjrood-Joolab	Many houses in Amol, Babol, Sari and Behshahr destroyed, liquefaction in river valleys happened
7	1825	Haraz valley	Many villages and all bridges and tunnels in Haraz road destroyed
8	1830	South Mazandaran	Shemiranat and Damavand region in east of Tehran completely destroyed
9	1890	Koohshangi-Shavoor	Many houses between Gorgan and Shahood destroyed, caused many aftershocks for 5 months
10	1935	Talar River	8 villages destroyed
11	1935	Goleijan-chahar Dangeh	Many villages destroyed, caused some destructive aftershocks for 24 h and after that some moderate aftershocks for 6 months
12	1957	Bandpey	Over 25,000,000 \$ economical toll

**Fig. 7** Study region located in 3 major seismotectonic provinces

of Alborz mountains to south of Mazandaran littoral plain. As shown in previous research, the earthquake that occurred in 874 with  $M_s = 6$  and the earthquake that occurred on 5 April 1994 with  $m_b = 5.2$  are attributed to this fault's activity.

**Alborz fault:** This fault has the length is equal to about 550 km from Lahijan to south of Gonbad-e Kāvus in north mountainside of Alborz mountains. It is probable that many earthquakes that occurred in Gilan and Mazandaran provinces are the results of this fault's activity.

**Seismic range of Gonbad-e Kāvus** In the current study, the required database of earthquakes is accumulated from

**Table 2** Relationships between  $M_s$  and  $M_b$  for seismotectonic provinces

Seismotectonic province	Magnitude intervals	Relationship
Alborz-Azarbayejan-Kopeh dagh	$4 < m_b < 6.2$	$M_s = 2.01m_b - 5.28$
Central-East Iran	$4 < m_b < 6.2$	$M_s = 2.0m_b - 5.28$

different sources, such as IIEES, USGS and Ngdir websites and the catalog of earthquakes prepared by Ambraseys and Melville (2005). As related to information accuracy, these earthquakes have been divided into three categories, as follows:

1. Historical earthquakes that occurred before 1900.
2. Instrumental earthquakes that occurred between 1900 and 1964 (recorded by analog instruments and inaccurate).
3. Instrumental earthquakes that occurred after 1964 up to now (recorded by digital instruments and accurate).

Earthquake magnitude is one of the most important parameters to identify the strong ground motion. According to the catalog of earthquakes, it is common to acquire different species of magnitude scales such as  $M_s$ ,  $M_b$  or other scales of magnitudes. Based on the note that the catalog has to be uniformed in seismic hazard analysis, all magnitude scales should be transformed to a single scale like  $M_s$ . For this purpose, the initial strive is to acquire a correlation between  $M_s$  and  $M_b$  by considering information that is provided by earthquake catalog of the studied region. However, there are few earthquakes with two



different species of announced magnitude scales that constitute the consequence of this striving unreliable. As a result, by using the correlations presented by Mirzaei (1997) in Table 2  $M_b$  is converted to  $M_S$ . Also, to convert other magnitudes to  $M_S$ , correlations are presented by Green and Hall (1994) is used.

#### *The estimation procedure of seismic hazard*

According to previous research, seismic hazard assessment can be conducted by three different ways:

1. A deterministic approach that is based on historical data when a particular scenario is assumed. This method is named DSHA (deterministic seismic hazard analysis) and shares the main aim of some recent seismic hazard studies, i.e., the studies carried out in Greece, Turkey and for critical infrastructures in California.
2. A probabilistic approach in which uncertainties in earthquake size, location and time of occurrence are the main purposes of a study.
3. A hybrid method that involves the advantages of both deterministic and probabilistic methods.

For the first time, Cornell et al. (1968) defined the traditional methodology of probabilistic seismic hazard analysis. Mainly given the insufficient earthquake data available in potential seismic sources, this methodology meets with problems in practice. To eliminate these shortcomings and also in order to properly reflect inhomogeneity of seismicity in time and space, the traditional methodology was modified by Chinese experts (Shi et al. 1992). This method includes three major steps which are presented below:

1. Delineation of seismotectonic provinces and evaluation of seismicity parameters (i.e.,  $b$  value, annual mean occurrence rate ( $\lambda$ ), and maximum possible magnitude,  $M_{\max}$  in each seismotectonic province.
2. Determination of potential seismic sources that includes estimation of  $M_{\max}$  in the potential seismic sources and evaluation of spatial distribution function for each magnitude interval in each potential seismic source.
3. Dividing the region into a series of grid points and assessment of seismic hazard for every grid point, using characteristics of seismic activity in seismotectonic provinces and potential seismic sources through an earthquake ground motion attenuation relationship.

In this numerical study, the modified methodology of probabilistic seismic hazard assessment (PSHA) is used to prepare seismic acceleration spectrum charts of Golestan area. For this purpose, after delineation of major

seismotectonic provinces surrounding the study area, a uniform catalog of earthquakes including historical and instrumental events covering the period from seventh century A.D. to 2012 is used and also 25 potential seismic sources are modeled as area sources in the region. Seismicity parameters are evaluated by using the method in which magnitude uncertainty and incompleteness of earthquake data are considered. Seismic hazard assessment is done for a grid of 300 points with 0.15 (degree) intervals using the SEISRISKIII computer program. According to modified methodology of probabilistic seismic hazard analysis, the present study makes available more reliable seismic hazard evaluation for Golestan region. The corresponding results are presented by acceleration spectrum charts with 10 and 2 % PE in 50 years for soft soil.

#### *Determination of the geometry and location of potential seismic sources*

It is of note that, seismological indications are the main parameters to choose potential seismic source regions. Seismic source zones can be determined by using tectonic information of the region and epicenter distributions of earthquakes together with other available geological and geophysical information. In this work, 25 area sources are delineated in the “Golestan” region as shown in Fig. 8.

#### *Attenuation relationship*

Attenuation relationship has a prominent role in probabilistic seismic hazard analysis. Note that, attenuation relationship defined the correlation of ground motion parameters with magnitude, distance and in some cases other parameters. Moreover, they are affected by many factors; the most important factors are presented below:

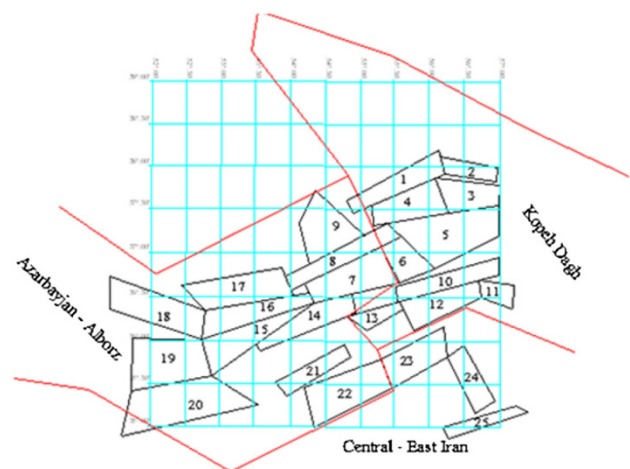


**Fig. 8** Seismic sources of the region





**Table 3** Spatial distribution functions and  $M_{\max}$ 

Source	$M_{\max}$	$5.5 < M_s < 6$	$6 < M_s < 6.5$	$6.5 < M_s < 7$	$7 < M_s < 7.5$	$7.5 < M_s < 8$
1	7		0.0017	0.0009		
2	7		0.0016	0.0008		
3	7.7		0.0017	0.0009	0.0003	0.0001
4	7		0.0018	0.0009		
5	7		0.002	0.0009		
6	6.5		0.0014			
7	7.5		0.008	0.0028	0.0012	
8	7.5		0.0065	0.0023		
9	6.5		0.0057			
10	7		0.0015	0.0009		
11	6.5		0.0014			
12	7		0.00180	0.0009		
13	6.5		0.0015			
14	7.9		0.0064	0.0025	0.001	0.0003
15	7		0.0071	0.0028		
16	7		0.0073	0.0029		
17	7		0.0065	0.0025		
18	7.5		0.0077	0.0029	0.0011	
19	7.5		0.0082	0.0029	0.0012	
20	7.5		0.0069	0.0025	0.0011	
21	6.5		0.0055			
22	7		0.0082	0.0031		
23	6.5	0.0028	0.0010			
24	6.5	0.0026	0.0009			
25	7	0.0035	0.0013	0.0002		

- Source specifications, magnitude, fault rupture type and distance to the seismogenic sources.
- Wave path, reflection, refraction and energy absorption due to the properties of materials through which the waves pass.
- Geology and topology of site.

Selection of proper attenuation relationship is a vital step to validate the analysis results. Therefore, in the current study, a worldwide attenuation relationship proposed by Ambraseys et al. (2005) is used. In this attenuation relationship, the functional form is as shown in Eq. (1):

$$\begin{aligned} \log y = & a_1 + a_2 M_w + (a_3 + a_4 M_w) \log \sqrt{d^2 + a_5^2} + a_6 S_S \\ & + a_7 S_A + a_8 F_N + a_9 F_T + a_{10} F_O, \end{aligned} \quad (1)$$

where  $y$  is the horizontal PGA,  $M_w$  is the moment magnitude,  $d$  is the surface projection of the source to site distance,  $S_S = 1$  for soft soil sites and 0 otherwise,  $S_A = 1$  for stiff soil sites and 0 otherwise,  $F_N = 1$  for normal faulting earthquakes and 0 otherwise,  $F_T = 1$  for thrust faulting earthquakes and 0 otherwise and  $F_O = 1$  for odd faulting earthquakes and 0 otherwise.

#### Seismicity parameters in the state of seismotectonics

*Estimating  $M_{\max}$  of potential earthquake sources* As mentioned above, the seismic sources are specified for the study area, the subsequent step is to specify the maximum earthquake magnitude for each seismic source that there are two ways to determine it:

1. The first method is the maximum historical earthquake procedure in which the maximum historical earthquake is enhanced by half a magnitude unit, or specified through a recurrence relationship.
2. The subsequent method is the fault rupture length procedure that the most common feature is the surface rupture length in this method. Usually, length of fault segments is used for determining maximum magnitude earthquake in a seismic source zone according to previous research.

Even so, in the current study, as demonstrated in Table 3 final  $M_{\max}$  values in the potential seismic sources of the study region are specified by the two above methods and incorporated with together. Besides, one of the most commonly used models proposed by Wells and Copper-smith (1994) is chosen.



*Seismicity parameters in the potential seismic sources* The problems related to use the traditional procedure of probabilistic seismic hazard assessment proposed by Cornell (1968) in practice could be caused by inadequate earthquake data accessible in each potential seismic source. To overcome the problems, initially seismicity parameters of each seismotectonic province are determined and afterwards they are dedicated to each magnitude interval in the corresponding potential seismic source by using spatial distribution function. This method is applied in the current study.

*Annual mean occurrence rate of earthquakes in the potential seismic sources* In seismic hazard analysis, integration on magnitude–frequency relation is used to annual mean occurrence rate of earthquakes in potential seismic sources. However, this method cannot reflect spatial inhomogeneity of seismicity. Shi et al. (1992) introduced the concept of spatial distribution function for specified magnitude intervals to fulfill this problem, which reveals a more realistic activity rate of small and large-magnitude earthquakes in the potential seismic sources. In this method, seismotectonic province is considered as a statistical unit to evaluate the seismicity parameters (i.e.,  $b$  values and annual mean occurrence rate,  $\lambda$ ) and also the mean annual occurrence rate in seismotectonic province will be allocated to each magnitude grade in the corresponding potential seismic source. In practice, each potential seismic source inside a seismotectonic province is labeled,  $l$ , to indicate the location of the potential seismic source. The magnitude range ( $M_{\min} < m < M_{\max}$ ) will be divided into a series of same magnitude intervals, so that the central value of the  $j$ th magnitude interval is  $m_j$ . Note that the annual mean occurrence rate of the  $j$ th magnitude interval in a seismotectonic province is evaluated according to Eq. (2):

$$\lambda_{mj} = \frac{2\lambda \exp[-\beta(m_j - M_{\min})] \text{sh}[0.5\beta\Delta M]}{1 - \exp[-\beta(M_{\max} - M_{\min})]}; \quad M_{\min} \leq m_j \leq M_{\max}, \quad (2)$$

where  $\beta = b \ln 10$ ,  $b$  is the value in the frequency–magnitude relationship of the seismotectonic province,  $m_j$  is the central value of the  $j$ th magnitude interval,  $\text{Sh}$  is the hyperbolic sine function,  $\Delta M$  is the width of magnitude interval, and  $M_{\min}$  and  $M_{\max}$  are the minimum magnitude (usually  $M_S = 4.0$ ) and the maximum expected magnitude in the seismotectonic province, respectively.

For the  $l$ th potential seismic source in the seismotectonic province, the annual mean occurrence rate of the  $j$ th magnitude interval is according to Eq. (3):

$$\lambda_{l,m_j} = \frac{2\lambda \exp[-\beta(m_j - M_{\min})] \text{sh}[0.5\beta\Delta M]}{1 - \exp[-\beta(M_{\max} - M_{\min})]} f_{l,m_j}; \quad M_{\min} \leq m_j \leq M_{\max}, \quad (3)$$

where  $\lambda_{l,m_j}$  and  $f_{l,m_j}$  are the annual occurrence rate and spatial distribution function of the  $j$ th magnitude interval in the  $l$ th potential seismic source, respectively.

*The spatial distribution function* The annual mean occurrence rate of earthquakes in seismotectonic province can be dedicated to each magnitude interval in the corresponding potential seismic sources, using the spatial distribution function. This process contributes to avoid underestimation of potential hazard of large-magnitude earthquakes, and to properly reflect the inhomogeneity of seismicity in time and space. Different kinds of seismological, tectonic, and geophysical data can be used to demonstrate the possible future earthquake activities in the study region, providing basis for evaluation of spatial distribution function. In this context, in order to evaluate spatial distribution function, some controlling factors considered that are discussed as follows.

*The reliability of delineation of potential seismic sources* Note that the degree of reliability in delineation of potential seismic sources is different inside a seismotectonic province. For some sources, there are sufficient indications (such as geological, tectonic, seismicity, and so forth) to delineate source zone boundary reliably, while for others, boundaries are indicated from indirect indications (magnitude lineaments, geomorphology, and so forth). Therefore, the reliability of each potential seismic source is determined by sufficiency of knowledge in delineation of potential seismic source that is denoted by factor ( $k_1$ ).

*Tectonic setting of potential seismic sources* Seismicity activity is localized mainly in major fault systems along plate boundaries which are sites of plate interactions, whereas interpolate environments have more stability and strength than interplate regions. In other words, whether the potential seismic source is located along the plate boundary or in the interior of the plate, it is used as a key factor ( $k_2$ ) in the evaluation of possible relative activity in potential seismic sources.

*Structural elements* The extent and activity level of structural elements (i.e., faults, folds, magnetic lineaments, active basins, and so forth) may be used as basis to judge levels of future seismic activity for a selected magnitude interval. On the other hand, geological, tectonic maps and seismotectonic maps with available information of active tectonics and earthquake-related structures are used as a database to evaluate this factor ( $k_3$ ) in potential seismic sources of each seismotectonic province.



**Characteristics of seismic activity** Distribution of large and small earthquakes may not be the same in a seismotectonic province due to local differences in physical properties of the earth's crust. This feature is very important to quantify and reflect such differences of seismic activity in seismic hazard analysis. In general, there is no appropriate method to clearly recognize and quantify such differences. For this reason, this regional variation is generally accepted. In the current study, it is assumed that seismic history of the region may, in part, reflects differences of physical properties to incorporate this important element in seismic hazard analysis. Since incompleteness of the available data and uncertainties in different earthquake parameters recorded earthquakes cannot fully show such differences, it is worth nothing; therefore, in order to consider of this factor ( $k_4$ ) special attention should be paid to reliability of earthquake records.

**Analysis method** Yan (1993) presented the calculation of spatial distribution function based on the controlling factors that is formulated by the method of equal weight summation, as follows:

- A distribution coefficient  $W_{lmjk}$  is assigned for the selected factor  $k_i$ , in which  $i = 1-4$ , for each magnitude interval  $m_j$  in the  $l$ th potential source,
- According to Eq. (4), in each seismotectonic province the distribution coefficient is normalized to obtain the factor load:

$$Q_{lmjk} = \frac{W_{lmjk}}{\sum W_{lmjk}}, \quad (4)$$

- Loads of controlling factors in each potential source are used to define total load,  $R_{lmj}$ , which is simply the sum of factor loads, as shown in Eq. (5):

$$R_{lmj} = \sum Q_{lmjk}, \quad (5)$$

- The total load  $R_{lmj}$  is normalized in each province to obtain the spatial distribution function for the  $j$ th magnitude interval in the  $l$ th potential seismic source, as shown in Eq. (6):

$$f_{lmj} = \frac{R_{lmj}}{\sum R_{lmj}}. \quad (6)$$

Limitations associated with the use of these equations are: the selected factor  $k$  in our study changes from 1 to 4, and  $m_j$  is the magnitude intervals. The number of potential sources ( $l$ ) ranges from 1 to 25.

**Background earthquake** In the regions in which lack of information does not allow for delineation of potential

seismic sources, and even in areas where active faults are defined, it is necessary to model background earthquake (background seismicity). In the concept of background seismicity, small and moderate-sized earthquakes may occur in the defined area randomly. In this study, background earthquake values are defined as  $M_S = 6$  for Alborz-Azarbayejan and Kopedagh provinces and  $M_S = 5.5$  for Central-East Iran province.

#### Hazard assessment for Golestan region

So far, numerous seismic hazard forecasting models were developed by many researchers. In this regard, the amply used model is the Poisson model with the assumptions that seismic occurrences are spatially and temporally independent and the probability that two seismic occurrences will take place coincidentally approaches zero and at the same location. A usual presumption in most of the seismic hazard models is that seismic sources are homogeneous. This means that every point within the same source has identical probability of being an epicenter for a future earthquake. On the other hand, this presumption provides seismic hazard outputs leading to variation at the borders of seismic zones. In order to provide a smooth transition of probability of seismic hazard from the seismic source to the adjacent areas, the notion of “earthquake location uncertainty” is introduced by Bender and Parkins (Bender and Perkins 1987). They supposed that each point within the zone is considered as the mean or the most likely location of a future earthquake; the locations of actual earthquakes are normally distributed with standard deviation about their mean locations. Seismic hazard evaluation of Golestan with centrality of Kāvus for 10 % probability of exceedance (475 years return period) and 2 % probability of exceedance (2,475 years return period) is conducted for soft soil (type III); hereby, acceleration spectrum charts has been revealed for 10 and 2 % probability of exceedance in 50 years (Fig. 9).

#### Modal analysis

The modal analysis is the prerequisite for the spectrum analysis. In other words, the results of modal analysis can be used in the dynamic spectrum analysis. The notable point here is that the modal analysis is done in linear limits in ANSYS and even if nonlinear elements and features are defined, neither of them will be considered, and consequently dynamic analysis is done in linear limits. The graphical results of the modal analysis for the 10 main modes, including transitional and



**Fig. 9** **a** Spectral acceleration chart for Gonbad region for 10 % probability of exceedance in 50 years and soft soil (type III) by Ambraseys et al. (2005); **b** spectral acceleration chart for Gonbad region for 2 % probability of exceedance in 50 years and soft soil (type III) by Ambraseys et al. (2005)

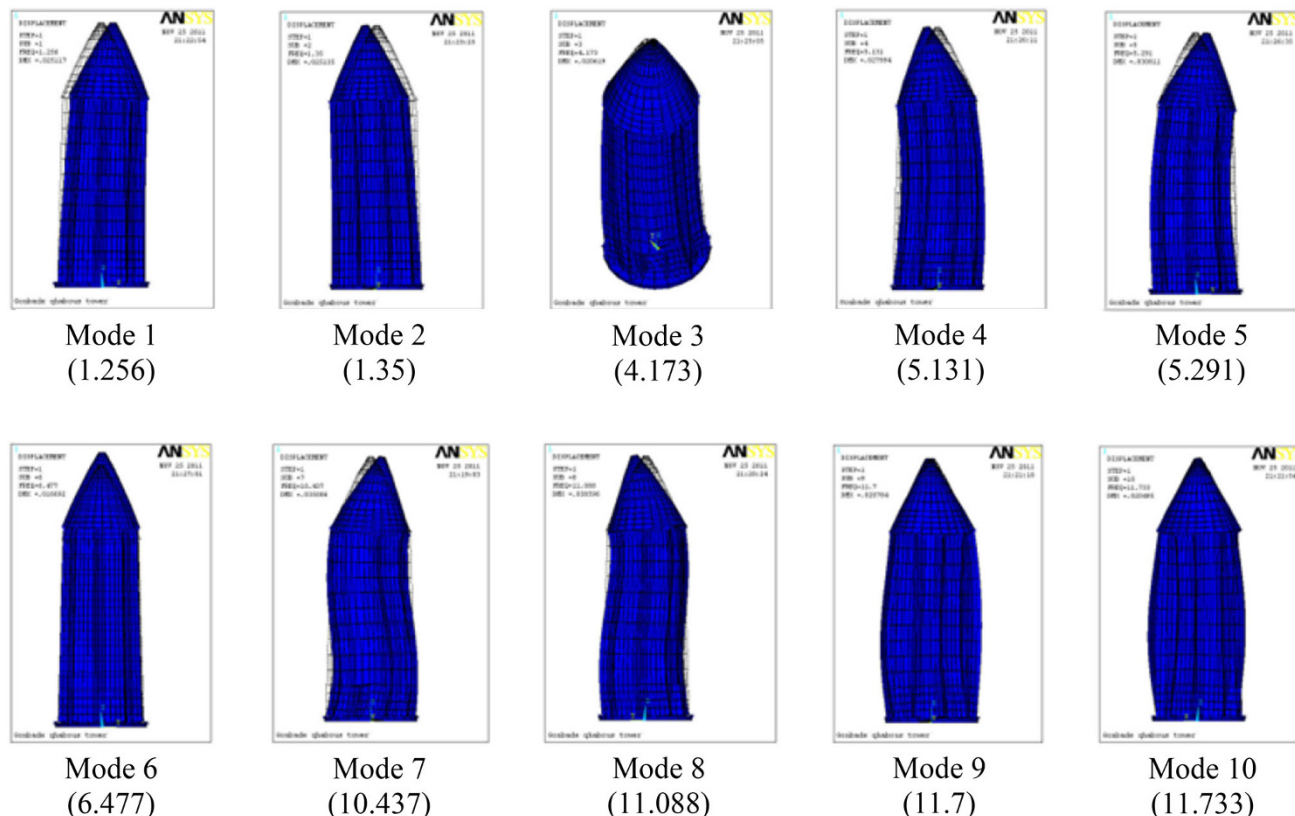
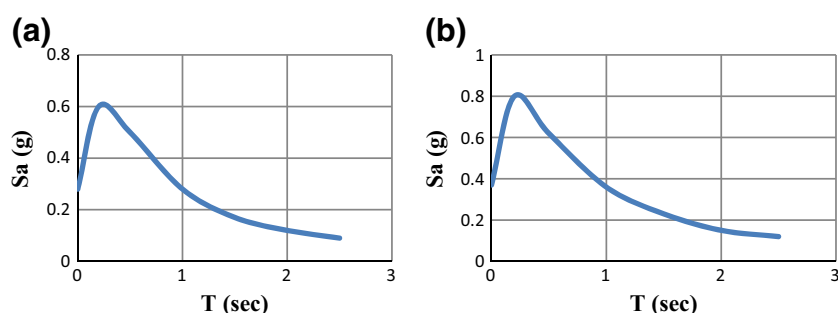


**Fig. 10** Mode shapes and the associated frequencies in Hz of the first 10 natural modes of vibration

rotational modes are mentioned in Fig. 10. According to Fig. 10, the period of the first mode has been equal to 0.8, and given that Iranian Seismic Code (2800) considered the upper limit of period ( $T_s$ ) equal to 0.7 for soil type III and also according to Eq. (7) that indicates reduction of structural stiffness is accompanied with increase the period of structure, whereby it can be concluded its behavior is soft and flexible

$$T_n = \frac{2\pi}{\omega_n} = 2\pi \sqrt{\frac{m}{k}} \quad (7)$$

**Table 4** Summary of the results of dynamic analysis using two spectra in X and Y directions

Period	Dir	S1 (tensile strength)	S3 (compressive strength)	SINT (shear strength)	$D_x$ (max displacement)
475	X	311.796	25.998	255.436	0.0075
	Y	348.366	20.273	305.266	0.0076
2475	X	462.02	39.017	378.536	0.0113
	Y	522.078	30.47	456.744	0.113





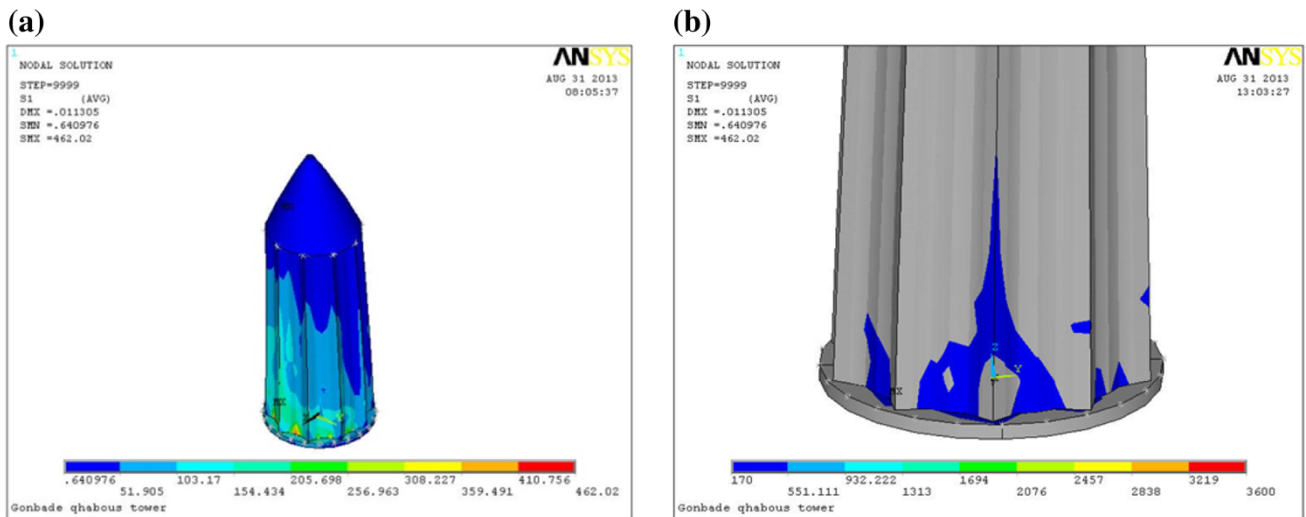


**Fig. 11** The earthquake spectrum with 2,475 years return time: **a** tensile stress in the behind view (S1, Dir X); **b** stress contour for X direction (tensile stress is more than the allowable tensile stress marked with blue)

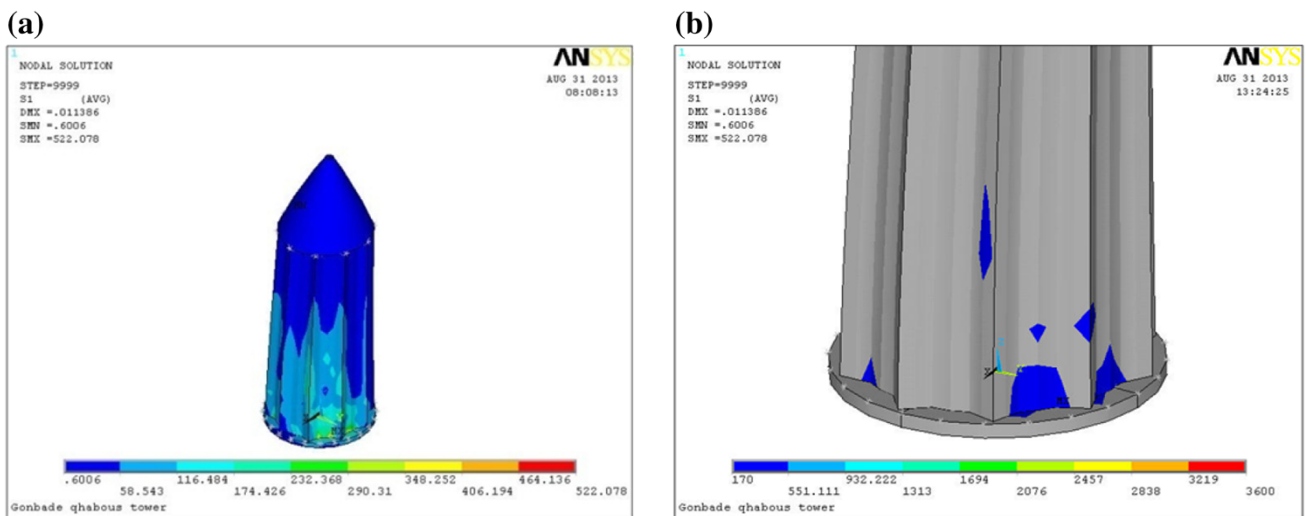


**Fig. 12** The earthquake spectrum with 2,475 years return time **a** tensile stress in the front and behind view (S1, Dir Y); **b** stress contour for Y direction (tensile stress is more than the allowable tensile stress marked in blue)

### Dynamic analysis

The dynamic analysis is not an exact analysis method meaning that its results are not the same as the time history analysis. But for many cases, the results are exact enough for designing the structure. Apart from this problem, there are some limitations for this method:

1. This method is applicable for linear analysis.
2. This method is not applicable for situations in which there are asymmetrical excitations in its supports.

Since the spectrum analysis is done linearly, for obtaining a logical conclusion for analysis of the results, study of the principle stress and comparing them with the

recommended allowable stress, the parts of the structure which are cracked and prone to compression failure have been discovered.

Therefore according to note 2-2-4-13 of the Iranian Seismic Code (2800), the number of seismic modes in each perpendicular direction of the building must take the following conditions into account, but only any of which is more in number: at least the three first modes, or all modes of vibrations with period times more than 0.4 s or all modes of vibration in which the sum of their effective masses are more than 90 % of the total mass of the structure. According to the results of modal analysis, there are 25 modes which their periods of time are more than 0.4 s. Since the period time of various modes of the

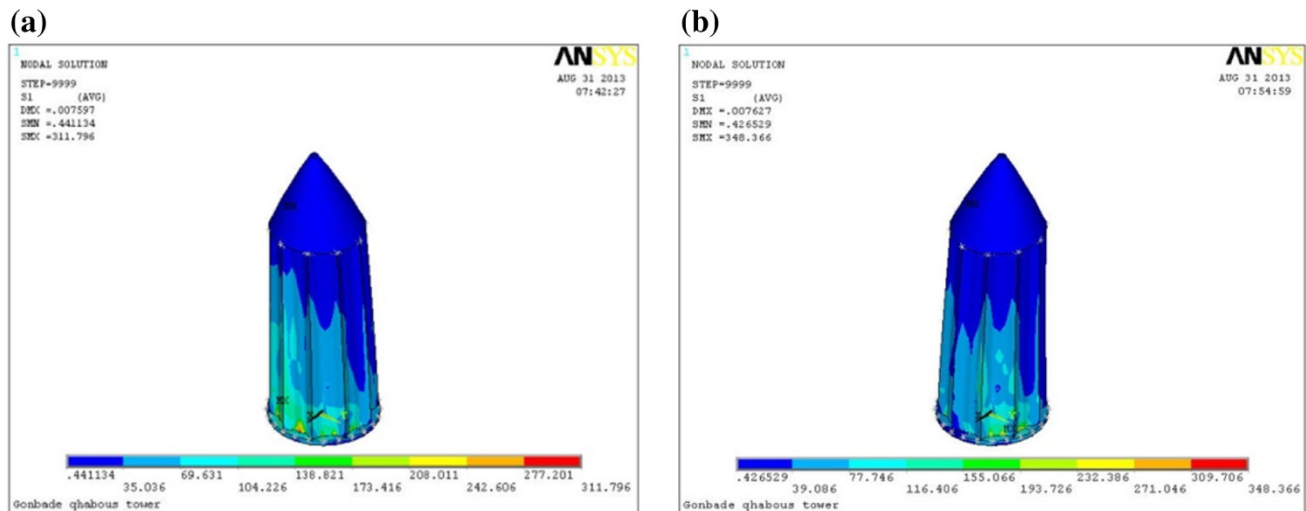


**Fig. 13** The earthquake spectrum with 475 years return time: **a** tensile stress in the behind view (S1, Dir X); **b** tensile stress in the behind view (S1, Dir Y)

structure are very close to each other and also they do not satisfy the Eq. (8), for combining the effects of different modes, the Complete Quadratic Combination (CQC) method is used.

$$r = \frac{T_m}{T_n} \leq 0.67; (T_n > T_m), \quad (8)$$

where the damping ratio is assumed as 5 % and  $T_n$  and  $T_m$  are period times for modes  $n$  and  $m$ , respectively.

In the current study, the spectrum analysis is shown by using two spectra that are obtained by risk analysis method with of 475 and 2,475 years return periods, and each of these spectra have been studied separately for both  $X$  and  $Y$  directions. In the following, the results of this analysis are studied and compared.

#### *Discussion on the result of the dynamic analysis under site-specific spectrum with 475 years and 2,475 years return period*

According to the results of spectrum analysis by using the site-specific spectrum with 475 and 2,475 years return period, the values of stresses and displacements obtained for both directions ( $X$  and  $Y$ ) are presented to Table 4. By comparing the values, it can be seen that Gonbad-e Kāvus tower has a good resistance against the two spectra obtained from risk analysis. However, according to Figs. 11a and 12a, in the lower parts of the body during an earthquake with probability of exceedance 2 % in 50 years, maximum tensile stress 522.078 and 462.02  $\text{KN/m}^2$  are generated in  $Y$  and  $X$  directions, respectively, that are greater than the allowable value (170  $\text{KN/m}^2$ ) seen at the backward facade of the structure. In this region, there is possibility of cracks in the direction perpendicular to the

tensile stress that it could endanger the stability of the structure. It can be concluded that the common methods of retrofitting brick buildings for the lower parts of the dome can be used to prevent cracking due to tensile stress. In order to better delineate the parts of the tower with tensile stress more than the allowable tensile stress using the earthquake spectrum with 2,475 years return time, a stress contour under the tensile stress S1 is presented in Figs. 11b and 12b. In these figures, the parts with tensile stress more than the allowable tensile stress are marked with blue (Figs. 11b, 12b). In addition, that of the maximum tensile stresses (i.e., S1) created by an earthquake with the 475 years return period in two directions of the structure are more than the allowable value (170  $\text{KN/m}^2$ ). However, we can ignore this in the backward view of the structure and in the connection point of the foundation and the body because it comprises very little surface area (Fig. 13). Also, by comparing the maximum compression stresses (i.e., S3) and shear stresses (i.e., Sint), in Table 4, with allowable values (i.e., 3,600 and 1,800  $\text{KN/m}^2$ , respectively) in the earthquake with 475 years and 2,475 years return period, it can be concluded that the maximum stresses that appear in both directions are less than the allowable values, so that these values indicate that the structure has enough resistance under shear and compression stresses and brick structures have good resistance under lateral forces.

#### **Conclusions**

In the current paper, seismic behavior of Gonbad-e Kāvus tower using the maps available at the organization of Cultural Heritage of Golestan Province by finite element software ANSYS is studied. Also the accuracy of model is



approved by gravity analysis, results of this analysis affirm that load transfer is done correctly among the elements, and the obtained weight is 86,400 KN.

Then probabilistic seismic hazard assessment has been performed for Gonbad region. In order to prepare the acceleration spectrum charts of the region, an area about 120 km is selected. Dividing the region to a grid of  $0.15^\circ$  in longitude and latitude and using the SEISRISK III computer software, seismic hazard assessment of 300 grid points has been carried out. Peak ground acceleration (PGA) and spectral acceleration (Sa) in  $T = 0.2, 0.5, 1.0, 1.5, 2.0, 2.5$  s for 2 % probability of exceedance (return period of 2,475 years) and 10 % probability of exceedance (return period of 475 years), in soil type III, have been estimated; consequently, PGA values are estimated to be 0.28 times gravity for 475 years return period.

Next step is modal analysis using spectral analysis; in this step, first period time is 0.75 s that indicates the structure is a soft construction. Then spectral analysis is done to identify the parts of the dome with stress more than the allowable stress. The results of spectral analysis in two X and Y directions for earthquake with 475 years period time show that the structure is resistant against used earthquake spectra well, just in some very small parts in the lowest part of dome, the maximum amount of tensile stress exceeds the allowable stress,  $170 \text{ KN/m}^2$ . However, this part can be ignored because it is too small and it cannot cause a serious threat to stability. But for earthquake with of 2,475 years period duration tensile stress in more part of the building exceeds the allowable stress,  $170 \text{ KN/m}^2$  and deeper cracks exist in the weak parts. In other words, earthquakes in this level can cause damage to the overall structure of the tower.

In general, according to historical analyses, the tower has good compressive resistance due to large load-bearing members of the structure, and tensile resistance identifies the weak parts. However, new technologies can suggest good ways to improve the seismic behavior of these culturally important buildings. There is hope that these efforts lead to the protection of valuable constructions that are the cultural and civil of signs of the country.

**Open Access** This article is distributed under the terms of the Creative Commons Attribution License which permits any use, distribution, and reproduction in any medium, provided the original author(s) and the source are credited.

## References

- Ahmadi GR, Mesbah A, Vetr MG (2012) Seismic vulnerability analysis and rehabilitation of Gonbad-e-Kavous Tower (The Tallest Brick Tower in the World). In: 15th International Conference on Earthquake. Lisbon
- Ambraseys NN, Melville CP (2005) A history of Persian earthquakes. Cambridge University Press, Cambridge
- Ambraseys NN, Douglas J, Sarma SK, Smit PM (2005) Equations for the estimation of strong ground motions from shallow crustal earthquakes using data from Europe and the Middle East: vertical peak ground acceleration and spectral acceleration. *Bull Earthq Eng* 3(1):55–73
- ANSYS (2007) Finite element analysis system, SAS IP Inc., US
- ANSYS (2007) Elements reference, release 11.0, SAS IP Inc., US
- Anthony J, Wolanski BS (2004) Flexural behavior of reinforced and prestressed concrete beams using finite element analysis. Faculty of the Graduate School, Marquette University
- Bartoli Gianni, Betti Michele, Giordano Saverio (2013) In situ static and dynamic investigations on the “Torre Grossa” masonry tower. *Eng Struct* 52:718–733
- Bayraktar Alemdar, Abdurrahman Şahin D, Özcan Mehmet, Yildirim Faruk (2010) Numerical damage assessment of Hagia Sophia bell tower by nonlinear FE modeling. *Appl Math Model* 34(1):92–121
- Bender B, Perkins DM (1987) SeisriskIII: a computer program for seismic hazard estimation. *US Geol Surv Bull* 1772
- Binda Luigia, Zanzi Luigi, Lualdi Maurizio, Condoleo Paola (2005) The use of georadar to assess damage to a masonry Bell Tower in Cremona, Italy. *NDT & E Int* 38(3):171–179
- Carpinteri A, Invernizzi S, Lacidogna G (2005) In situ damage assessment and nonlinear modelling of a historical masonry tower. *Eng Struct* 27:387–395
- Ceroni F, Pecce M, Voto S, Manfredi G (2009) Architectural, and structural assessment of the bell tower of Santa Maria Del Carmine. *Int J Archit Herit* 3(3):169–194
- Cornell CA (1968) Engineering seismic risk analysis. *Bull Seismol Soc Am* 58(5):1583–1606
- D’Ambrisi Angelo, Mariani Valentina, Mezzi Marco (2012) Seismic assessment of a historical masonry tower with nonlinear static and dynamic analyses tuned on ambient vibration tests. *Eng Struct* 36:210–219
- Datta TK (2010) Seismic analysis of structures. Wiley, Hoboken
- Ghodrati Amiri G, Razavian Amrei SA, Motamed R, Ganjavi B (2007) Uniform hazard spectra for different northern part of Tehran, Iran. *J Appl Sci* 7(22):3368–3380
- Green, Russell Andrew, William J Hall (1994) An overview of selected seismic hazard analysis methodologies
- Hejazi M, Nasri A (2009) Structural analysis of Dome Qaboos. In: 8th International Congress on Civil Engineering. Shiraz university, Shiraz (in persian)
- Instruction for seismic rehabilitation of existing unreinforced Masonry Buildings No.376 (2007) Technical Criteria Codification and Earthquake Risk Reduction Affairs Bureau (in persian)
- Iranian Network Management Services Company (irmeco) (2010) Seismic retrofit of experiences and lessons. Science and Literature Publishing (in persian)
- Ivorra Salvador, Pallarés Francisco J (2006) Dynamic investigations on a masonry bell tower. *Eng Struct* 28(5):660–667
- Kachlakev D, Miller T, Yim S, Chansawat K, Potisuk T (2001) Finite element modeling of concrete structures strengthened with FRP laminates: final report
- Kayabali K, Akin M (2003) Seismic hazard map of Turkey using the deterministic approach. *Eng Geol* 69(1–2):127–137
- Klügel JU, Mualchin L, Panza GF (2006) A scenario-based procedure for seismic risk analysis. *Eng Geol* 88(1–2):1–22
- Krinitzky EL (2003) How to combine deterministic and probabilistic methods for assessing earthquake hazards. *Eng Geol* 70(1–2):157–163
- Lourenço PB (2005) Assessment, diagnosis and strengthening of Outeiro Church, Portugal. *Constr Build Mater* 19(8):634–645



- Mavizchi M, Mavizchi M, Alemi F (2012) The vulnerability seismic assessment and providing reinforcement strategies for “Naj-moddin Kobra” historical monument. In: 15th International Conference on Earthquake. Lisbon
- Milani G, Casolo S, Tralli A, Naliato A (2012) Seismic assessment of a medieval Masonry Tower in Northern Italy by limit, nonlinear static, and full dynamic analyses. *Int J Archit Herit* 6:489–524
- Mirzaei N (1997) Seismic Zoning of Iran. Ph.D. dissertation in Geophysics, Institute of Geophysics, State Seismological Bureau, Beijing, People’s Republic of China, p 134
- Mirzaei Noorbakhsh, Gao Mengtan, Chen Yun-tai (1999) Delineation of potential seismic sources for seismic zoning of Iran. *J Seismolog* 3(1):17–30
- Modena C, Valluzzi MR, Tongini FR, Binda L (2002) Design choices and intervention techniques for repairing and strengthening of the Monza cathedral bell-tower. *Constr Build Mater* 16:385–395
- Moratto L, Orlecka-Sikora B, Costa G, Suhadolc P, Papaioannou Ch, Papazachos CB (2007) A deterministic seismic hazard analysis for shallow earthquakes in Greece. *Tectonophysics* 442(1–4): 66–82
- Mualchin L (2005) Seismic hazard analysis for critical infrastructures in California. *Eng Geol* 79(3–4):177–184
- Nakajima M, Choi IK, Ohtori Y, Choun YS (2007) Evaluation of seismic hazard curves and scenario earthquakes for Korean sites based on probabilistic seismic hazard analysis. *Nucl Eng Des* 237(3):277–288
- Nateghi-Alahi F, Alemi F (2008) Experimental study of seismic behaviour of typical Iranian urm brick walls. In: 14th International Conference on Earthquake. Beijing, China
- No, Standard (2005) 2800 Iranian Code of Practice for Seismic Resistant Design of Buildings”, Third Revision, Building and Housing Research Center, Iran (in Persian)
- Pace B, Boncio P, Brozzetti F, Lavecchia G, Visini F (2008) From regional seismic hazard to “scenario earthquakes” for seismic microzoning: a new methodological tool for the Celano Project. *Soil Dyn Earthq Eng* 28(10–11):866–874
- Peña Fernando, Lourenço Paulo B, Mendes Nuno, Oliveira Daniel V (2010) Numerical models for the seismic assessment of an old masonry tower. *Eng Struct* 32(5):1466–1478
- Repeated Author (2009) How to eliminate non-damaging earthquakes from the results of a probabilistic seismic hazard analysis (PSHA)—A comprehensive procedure with site-specific application. *Nuclear Engineering and Design* 239 (12):3034–3047
- Riva Paolo, Perotti Federico, Guidoboni Emanuela, Boschi Enzo (1998) Seismic analysis of the Asinelli Tower and earthquakes in Bologna. *Soil Dyn Earthq Eng* 17(7–8):525–550
- Shabani E, Mirzaei N (2007) Probabilistic seismic hazard assessment of the Kermanshah-Sanandaj Region of Western Iran. *Earthq Spectra* 23(1):175–197
- Shi Zhenliang, Yan Jiaquan, Gao Mengtan (1992) Research on the principle and methodology of seismic zonation. *Acta Seismol Sin* 5(2):305–314
- Tasmini A (2005) Behavior of the brick buildings with or without Skein Disaster Research Center, Tehran (in Persian)
- Tavakoli B, Ghafory-Ashtiani M (1999) Seismic hazard assessment of Iran. *Ann Geophys* 42 (6)
- Wells DL, Coppersmith KJ (1994) New empirical relationships among magnitude, rupture length, rupture width, rupture area, and surface displacement. *Bull Seismol Soc Am* 84(4):974–1002
- Architectural and Historical background and of Gonbad-e Kāvus Tower. Pictures and maps gathered from Golestan Cultural Heritage
- IIIES: International Institute of Earthquake Engineering and Seismology. <http://www.iiies.ac.ir>
- Ngdir: National Geoscience Database of Iran, <http://WWW.ngdir.ir>
- USGS. US Geological Survey, <http://WWW.USGS.gov>
- Whc.unesco: World Heritage Convention. United Nations Education, Scientific and Cultural Organization, <http://whc.unesco.org/en/statesparties/IR>
- Yan J (1993) Principals and methods to determine spatial distribution function. In: Proceedings, PRC/USSR Workshop on Geodynamics and Seismic Risk Assessment. Beijing, pp 159–167

